16 (2022) 100245

Contents lists available at ScienceDirect

International Journal of Thermofluids

journal homepage: www.elsevier.com/locate/ijtf

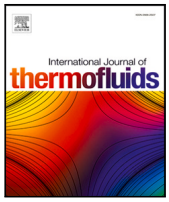

Numeric study of geothermal borehole heat exchanger enhancement via phase change material macro encapsulation

João Pássaro [a,b,*], A. Rebola [a], L. Coelho [a], J. Conde [b]

[a] Centro de Investigação em Energia e Ambiente, ESTSetúbal, Instituto Politécnico de Setúbal, Campus do IPS – Estefanilha, Setúbal, 2910-761, Portugal
[b] Universidade Nova de Lisboa, Caparica, Almada, 2829-516, Portugal

ARTICLE INFO

Keywords:
Macro-encapsulated phase change material
Ground sourced heat pump
Latent heat storage system
Ground thermal stabilisation
CFD melting/solidification model

ABSTRACT

This article addresses the theoretical effect of using geothermal boreholes enhanced with macro-encapsulated phase change materials (PCM) employed with a ground sourced heat pump (GSHP). The aim being the improvement of the heat pump performance through soil temperature stabilisation, taking advantage from the PCM inherent property of changing phase at a constant temperature, that can be matched with the temperature of the surrounding soil, contributing as well to increase the energy storage capacity underground. The numeric work studied different PCM thermal parameters with regards to their influence on the overall behaviour of the heat pump, with different operation modes (On/Off and Inverter) changing the solidus and liquidus temperatures and phase change enthalpy values. The CFD results showed that, while it underperformed having 0.15% difference in the best of cases (specifically the On/Off mode), it used in the best case scenario only 30% of the stored energy in the PCM. The application of macro-encapsulation did provide a stabilising effect to the soil and heap pump operation as it was originally intended to do, helping reduce energy expenditure by the system. Significant modifications are needed in order to improve, both concerning geometry and encapsulation techniques to overcome the PCM and other materials thermal limitations.

1. Introduction

Climatic change requires new innovations to reduce thermal energy needs in buildings. To this effect, the Energy Efficiency Directive was revised along with other regulations concerning climate and energy. This ensures that the new goals for 2030, for greenhouse emissions, will be met by at least 55% [1]. To this end, accelerated development of renewable applications is a must within all areas of energy usage. Nevertheless cyclical availability and influence by atmospheric conditions can cause limitations. These limitations could be minimised using other technologies such as thermal storage, storing energy for whenever the sun is not available [2,3]. Thermal storage has gained traction in the last few decades [4–6], helping to provide a smoother integration of renewable energy sources into residential and industrial buildings.

A different, renewable solution to provide space cooling and heating that works year-round regardless of other conditions is geothermal energy. Ground heat is a resource that is available worldwide, regardless of climate, with regional variations, and has been in use for a long time, becoming a well-known technology, with known benefits [7]. Despite its costs [8], performance wise, it is preferable for the installation to be made vertically as a greater depth provides better thermal stability [7,8]. For vertical installations there are various possible layouts of the piping circuitry, which are usually divided into two categories: coaxial and U-shaped. There is a variation for the coaxial arrangement called “Complex Coaxial” as well as a variation for “U” called, “Double U” or “UU”. For the U variations the pipe diameters range from 20–40 mm and the pipes are usually spaced 100–150 mm apart. The boreholes themselves also may vary between 100 and 200 mm for both coaxial and U variations, and the boreholes are usually up to 200 m deep [9]. The fill back grout material is the interface between the heat transfer fluid of the heat pump, and in this case, the stored PCM being employed. In and of itself it has, in part, the same issues of the of PCM as in that its thermal conductivity is the main issue when the system is operating. However, there are improvement methods employed, for example using particles dispersions with varied materials and sizes, aiming to increase the thermal transfer coefficient. Other approaches combine PCM directly with the grout materials to increase its thermal storage capacity. This last approach was discarded was it did not guarantee PCM not leaking to possible phreatic water tables and contaminating fresh water sources [10,11]. This system works by

* Corresponding author at: Centro de Investigação em Energia e Ambiente, ESTSetúbal, Instituto Politécnico de Setúbal, Campus do IPS – Estefanilha, Setúbal, 2910-761, Portugal.
E-mail address: jpap87@gmail.com (J. Pássaro).

https://doi.org/10.1016/j.ijft.2022.100245
Received 15 June 2022; Received in revised form 17 October 2022; Accepted 6 November 2022
Available online 17 November 2022

coupling a heat pump exchanging heat with the soil via boreholes that can have both a vertical or horizontal disposition. This technology does have a significant limitation because of the soil's low thermal diffusivity, which means there is a slow thermal response, decreasing the Coefficient of Performance (COP) for the heat pumps. To increase the borehole's thermal capacity, phase change materials (PCMs) can be added to the grout material used to backfill the drilled hole [5,12,13]. In this context, Aljabr et al. showed that to reach the optimum mass of PCM for borehole grout due to the competing factors of PCM thermal conductivity and its latent heat capacity effectively, the PCM thermal conductivity should be approximately equivalent to that of the grout material. Furthermore, the melt temperature of the PCM was found to be that which results in almost all of the PCM mass to change phase at the time of peak load. That temperature was found to be about midway between the undisturbed ground temperature and the peak design heat pump entering fluid temperature [5]. PCMs have shown a great potential due to their high heat capacity associated with relatively low volume. In this context, it has been observed that specific materials can absorb or release large amounts of energy while under certain operating conditions. These materials are capable of storing around five to 14 times more energy per unit volume than materials that store sensible heat, e.g.: water, concrete, or rocks, and having constant specific phase change temperatures [13]. In order for PCMs to be selected as TES materials some features are important to be met, while not limited to them, some of the most important are: good thermal conductivity, high latent heat of fusion and density, small volume phase change, chemical stability, non super-cooling, and cost effective, and more [14]. One notable issue with these materials is the fact that as a rule they have low thermal conductivity, compromising heat transferring capacity, which is the cornerstone of latent storage applications. To this end, research is needed to determine how to best adapt these materials to specific applications. Within this framework, energy storage for maintaining building temperature is an example of where PCMs can be used for thermal storage and temperature stabilisation [15,16]. Mousa et al. simulations showed that the use of multiple PCM melting temperatures led to a performance enhancement of up to 26% [17]. Another numeric study found that by employing PCM the total heat storage capacity increases over time with an increment about 90% occurring within 5 h [18], although this particular disposition was horizontal. Another source implemented shallow flat-panels ground heat exchanger in the backfill material, this application showed that PCMs can compensate peak loads occurring during hard weather conditions [19]. Alkhwildi et al. developed a parametric model for low temperature energy storage where a preliminary economic analysis suggested that with typical drilling cost and PCM tank cost values, the ground heat exchanger size can be reduced by over 50%, implementing a parallel tank with PCM for storing energy [6].

While there are several sources addressing ground heat source heat pumps and their heat exchangers, other concerning CFD and PCMs, there are limited literature sources addressing combination of both ground heat exchangers and Computational Fluid Dynamics (CFD) [20] as depicted here. While experimentation is very important, given the nature and cost of the studied processes it has serious limitations, being either impossible to effectively test a borehole heat exchanger if scaled down, or prohibitively costly to test it out at full scale. This is where CFD tools come into play, enabling full scale testing without its significant drawbacks concerning costs and installation. In this works specific example the heat pump operation mode is heating; however, the studied principles are transferable should the process be cooling, with the respective changes concerning the PCM characteristics. The results presented in this article show good agreement with recent literature showing how employing PCMs in ground-sourced heat exchanger applications can improve the performance of the system, and how the PCMs' thermal properties, such as latent heat capacity, are of importance [12,21]. Since there are few literary works that combine vertical geothermal boreholes, numeric work and PCMs this work brings a new insight into a potential application.

The objective of this work is to develop a proof of concept basis for a practical application that employs PCM in a ground-sourced heat pump (GSHP) coupled system. The emphasis here is to use one of the standard typologies of borehole heat exchangers, in this case Double "U", and alter it with minimum modifications. This would work twofold, combining a simple alteration of the current system without alterations that could make this already expensive application even pricier. If successful this application would help decrease the installation cost of this type of GSHP system by cutting down the depth of the boreholes, which are responsible for a significant fraction of the cost of the installation. Furthermore, using PCM in this context would also increase the energy storage capacity of the system, improving on the functionality overall of the system and its energy savings.

2. Numeric model

In the present study, nine simulation cases were studied to evaluate the influence of specific thermal parameters on the overall behaviour of a borehole coupled with a ground-sourced heat pump. These parameters examined the effect of the type of the heat pump operation such as On/Off or inverter technology with different operation schedules, and comparing them with and without PCMs. Furthermore, the effect of different PCM latent heat capacities was examined and how it impacted the systems behaviour, and the outcome of changing the work temperature of the PCMs comparatively with the soil temperature.

2.1. Simulated domain and materials

The employed borehole typology was a modified Double "U", despite being a Double "U" type borehole, only one circuit has close-looped water circulation; the other circuit was filled with PCMs to act as thermal storage. The borehole itself is 150 mm in diameter, with each of the four tubes having a diameter of 40 mm, evenly spaced out. The borehole has a depth of 90 metres. The soil portion of the domain is 6 metres in diameter as illustrated in Fig. 1.

The materials employed in all cases were: soil, fill back grout material, high density polyethylene, water and PCMs. Material properties are presented in Table 1. Four different PCMs were considered; these however, were not standard issue, meaning that the specifications and material properties were not drawn from a manufacturer catalogue. The properties of the PCMs were themselves studied to help understand how they influence the behaviour of the system. The specific characteristics were: the solidus and liquidus temperature and the phase change latent heat relative to the specified soil temperature, with the remaining properties used based on common organic paraffin waxes. It should be noted that the soil properties mentioned were generalised values, as soil properties vary greatly with geological locations, with possible heterogeneity throughout its depth with varying degrees of geological features (i.e. local water tables, voids of different sizes, density and material variations, etc.).

2.2. Mathematical model

The PCM solidification was simulated by the enthalpy-porosity formulation, the ability of this approach to model the solidification process of PCMs has been demonstrated in the past [22–24]. The complete numerical model solves the mass, momentum and energy transport equations for constant density. The viscous dissipation term is considered negligible while the energy equation is solved in the form of total enthalpy.

$$\frac{\partial \rho}{\partial t} + \nabla \cdot (\rho \vec{v}) = 0 \tag{1}$$

$$\frac{\partial}{\partial t}(\rho \vec{V}) + \nabla \cdot (\rho \vec{V} \vec{V}) = -\nabla p + \mu \nabla^2 \vec{V} + \rho_o \beta (T - T_o)\vec{g} + \vec{S} \tag{2}$$

Table 1
Material properties.

Property	Grout material	Soil	High density - polyethylene	Water	PCM
ρ [kg/m^3]	2250	1400	950	998	800
Cp [J/kg K]	1250	1000	2000	4180	2400(s)-1800(l)
k [W/m K]	2.35	2.00	0.42	0.60	0.24
α [m^2/s]	–	–	–	0.14e^{-7}	–

s — Solid phase l — Liquid phase.

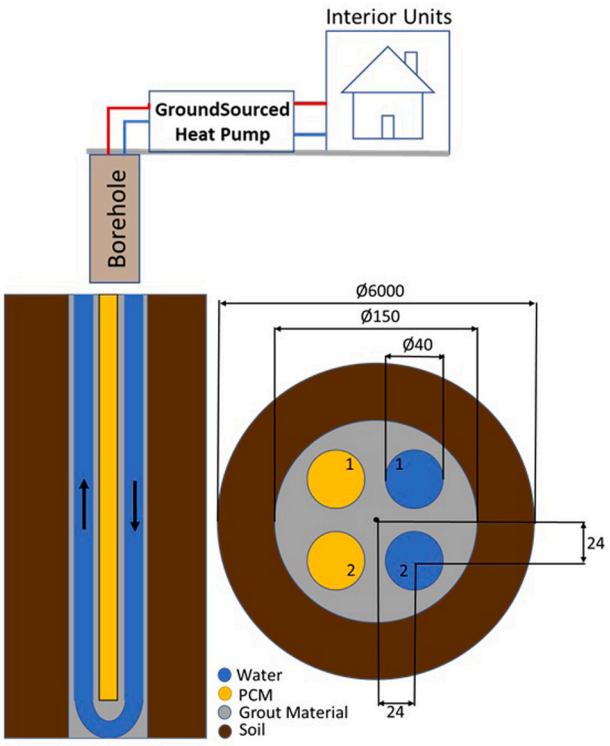

Fig. 1. General schematic of the application and 3D geometry measurements of the studied domains for modified "double U" configuration, in millimetres (drawing not to scale).

$$\frac{\partial \rho H}{\partial t} + \nabla \cdot (\rho \vec{V} H) = \nabla \cdot (k \nabla T) \tag{3}$$

V represents the velocity, ρ the density, μ the dynamic viscosity, k the thermal conductivity, T the temperature and H the total enthalpy, defined as:

$$H = h + \Delta H \tag{4}$$

$$h = h_{ref} + \int_{T_{ref}}^{T} C_p \, dT \tag{5}$$

h represents the sensible enthalpy, C_p the specific heat and ΔH the phase change enthalpy. The temperature is calculated through the total enthalpy and the liquid mass fraction γ defined as:

$$\gamma = \begin{cases} 0 & , T < T_{solidus} \\ \frac{T - T_{solidus}}{T_{liquidus} - T_{solidus}} & , T_{solidus} < T < T_{liquidus} \\ 1 & , T > T_{liquidus} \end{cases} \tag{6}$$

Locally, the phase change enthalpy can be written in terms of the liquid mass fraction and the PCM latent heat, L, as, $\Delta H = \gamma L$. The enthalpy-porosity formulation treats different phases as a porous media by means of the following source term $\vec{S}$:

$$\vec{S} = \frac{(1-\gamma)^2}{(\gamma^3 + \xi)} A_{mushy} \vec{V} \tag{7}$$

A_{mushy} is the mushy zone constant which describes how steeply the velocity is reduced to zero when the material solidifies. This is usually a very large value, ranging between 10^4 and 10^8 kg/(m^3 s), in the present study a standard value of $A_{mushy} = 10^5$ is employed. The constant ξ is a small value, in this case 10^{-3}, introduced to prevent division by zero.

2.3. Boundary conditions and initialisation

The temperature input on inlet was configured based on different compressor operation modes and operation duration of the GSHP. The heating operation modes were for an On/Off heat pump and an inverter heat pump. The On/Off mode relies on the heat pump power to fill the thermal needs regardless of how much is needed per time interval; the inverter mode allows for the power supplied to better match with the specific needed values over time. Originally, the time frame that was considered was a 24 h period for both operation modes but considering the soil inertia influence on the operation of the system, an additional input was selected based on a 48 h period for the inverter operation mode, also providing a different insight with a different work schedule. This schedule makes for a more intense usage over the first 18 h followed by a simulated absence with little usage up to the 48 h mark. Fig. 2 illustrates the heat rates that provided the temperature values for the inlet User's Defined Function (UDF) input.

The simulations time profiles (24 h and 48 h) employed heating operation modes and were tested for a geothermal system with the heat pump having a COP of 4. The average temperature of the soil considered was 17.5 °C and the HTF mass flow rate was 0.475 kg/s. For each time instant the inlet temperature of the HTF into the borehole was calculated based on the heat pump evaporator energy balance, expressed by an equation that would be employed in Inlet 1 depicted in Fig. 3, for the water pipe "1" Eq. (8).

$$T_{inlet}^{t} = T_{outlet}^{t-1} - \frac{\dot{Q}}{\dot{m} \cdot Cp} \tag{8}$$

The solution was initialised with the hybrid initialisation with the default features. The hybrid initialisation employed a collection of recipes and boundary condition interpolation methods, solving Laplace's equation to determine the velocity and pressure fields. All other variables including temperature, turbulence, species, volume fractions, etc. were automatically patched on domain averaged values or a particular interpolation recipe. The initialised model was then temperature patched with the studied soil average temperature (17.5 °C) on all domains.

2.4. Studied cases

The considered simulation cases can be seen in Table 2, making it possible to test out the influence of a generic paraffin wax based PCM (PCM A) that was selected, in some cases with a different latent heat and phase change temperatures (PCM B, C and D) to verify how each specific characteristic would impact the objective of the work developed in this section.

Table 2
Cases features.

Case ID	Heat pump operation	PCM type	PCM solidus temperature [°C]	PCM liquidus temperature [°C]	PCM latent heat [kJ/kg]	PCM energy capacity [kWh]
1	24 h – On/Off	–	–	–	–	–
2	24 h - Inverter	–	–	–	–	–
3	48 h – Inverter	–	–	–	–	–
4	24 h – On/Off	PCM A	15.5	16.5	200	10.05
5	24 h – Inverter	PCM A	15.5	16.5	200	10.05
6	48 h – Inverter	PCM A	15.5	16.5	200	10.05
7	48 h – Inverter	PCM B	15.5	16.5	150	7.54
8	48 h – Inverter	PCM C	15.5	16.5	250	12.57
9	48 h – Inverter	PCM D	16.0	17.0	200	10.05

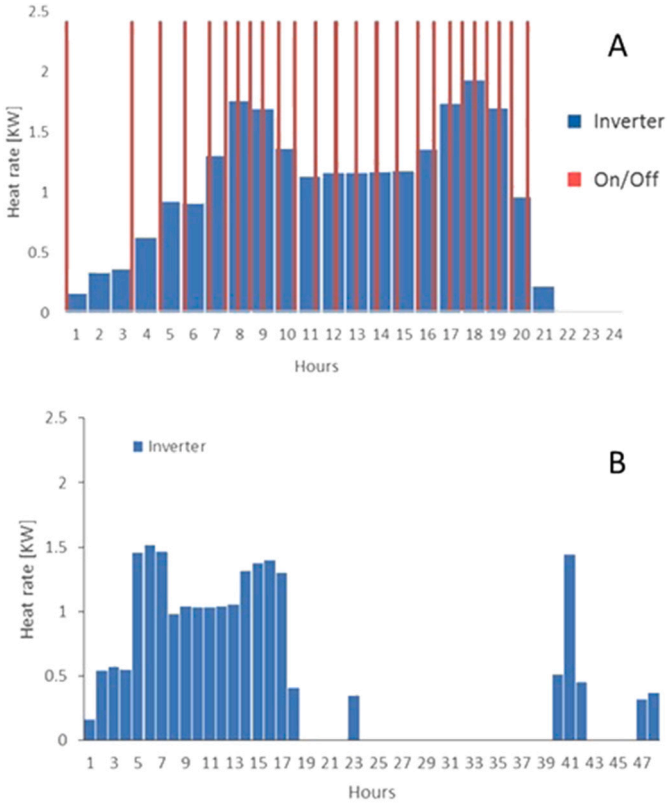

Fig. 2. Energy demand profiles for 24 h On/Off and inverter for same period (A) and 48 h Inverter operation (B).

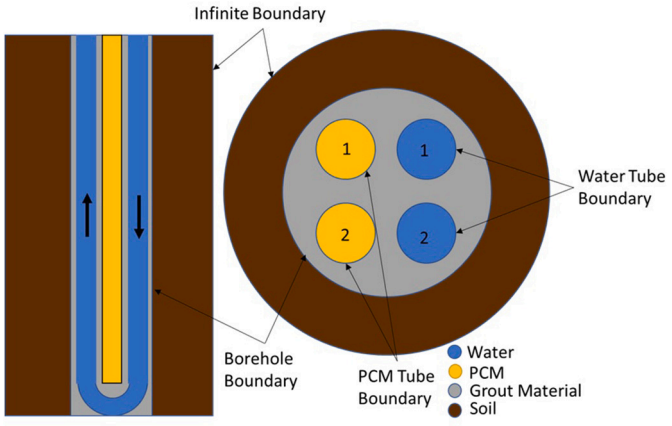

Fig. 3. Geometry the domain zones of the model and boundaries.

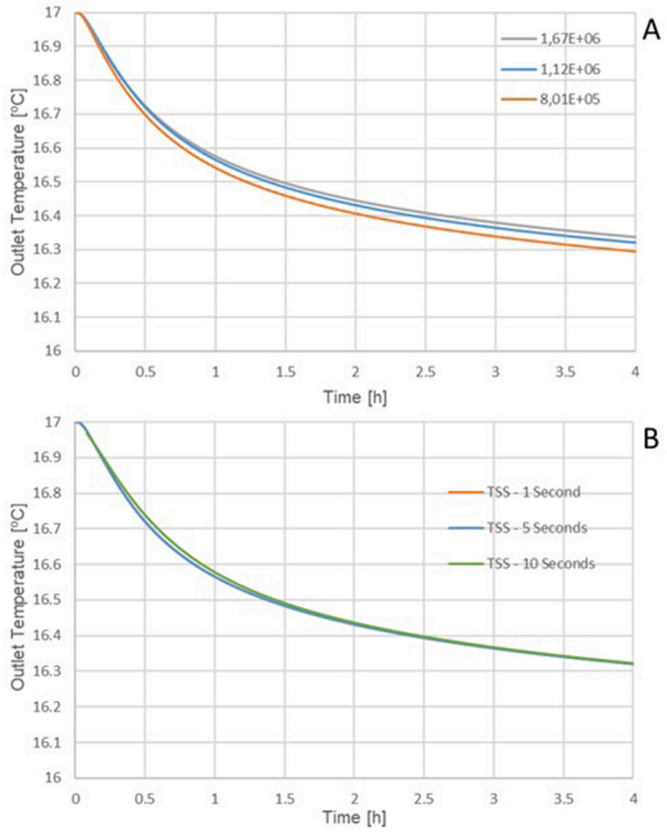

Fig. 4. Mesh size independence [A] and time step size independence verification [B].

2.5. Mesh and grid independence

The mesh was tested for independence with three distinct sizes, 8.01e5, 1.12e6 and 1.67e6 elements. The behaviour of the outlet temperature for each of the meshes can be seen in Fig. 4, image A All the values are within a small temperature range (between 16 and 17 °C), looking at graph A it can be seen that the grids with 1.12e6 and 1.67e6 elements have a greater precision. However, using the mesh with 1.67e6 elements would have a prohibitively long computational time for a minor gain in accuracy, thus the selected mesh for the studied cases was 1.12e6 elements. Likewise, the time step size independence was verified to ascertain the model precision, shown in Fig. 4, image B, illustrating three distinct time step sizes of 1, 5 and 10 s, and judging from the plots it can be seen that while one and five second time steps have the same results for the same mesh, the 10 s step has slightly lower accuracy, and since the step with one second had the same accuracy as the five second time step, the chosen Time Step Size was five seconds.

The model was built in a 3D grid with 1.12e10^6 hexahedral elements; the mesh being finer in the borehole region. Fig. 5 presents a

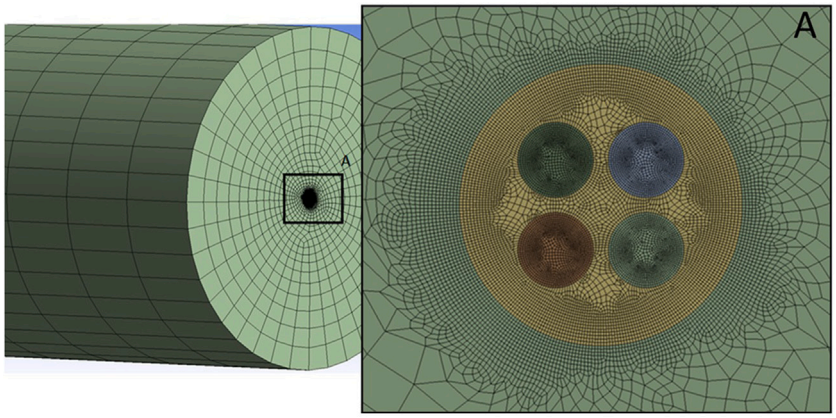

Fig. 5. Model grid and mesh detail [A].

detailed view of the computational mesh. In the longitudinal direction the mesh has 90 elements with the size of one metre. The soil volume mesh has an element size of five millimetres and within the PCM and water tubes the elements are two millimetres. Both the borehole and the PCM/water pipes have a layer of inflation added in the heat transfer surfaces.

2.6. Numerical methodology

For the numeric work the commercial code of Ansys FLUENT v17.0 was used, with the solver set to double precision. The pressure and velocity coupling of the model was set for the pressure equation through the SIMPLE algorithm with the PRESTO scheme, while the convention terms used the second order upwind discretisation, and the energy was discretised with the second order upwind scheme. The under-relaxation factor values were left as default for the pressure (0.3), density (1), body forces (1), momentum (0.7), turbulent kinetic energy (0.8), turbulent dissipation rate (0.8), turbulent viscosity (1) liquid fraction update (0.9) and energy (1). The convergence check for each time step was set to 10^{-3} for the continuity, momentum, and turbulence and the energy check was set to 10^{-9} to prevent false convergence from taking place.

3. Results and discussion

3.1. Case evaluation

The plotted lines displayed on Fig. 6 show how the different operating modes and cycles affect the behaviour of the borehole as a baseline. The figure shows, on the left, graphics for the temperatures of the heat transfer fluid inlet and outlet temperature. On the right, the temperature of the cylinders which would eventually house the PCM volume (see domains representations Fig. 3). It should be noted that, although in these three cases (1, 2 and 3) the volume is termed the "PCM Average Temperature" in the graphics, it is actually filled with grout material being later exchanged for actual PCMs for cases 4 through 9. Comparing the results from 1 and 2 it is clear that, while in the same time cycle the behaviour of the borehole is distinct. With case 1 the On/Off system has numerous and accentuated peaks and oscillations in the temperatures measured, reaching extreme low minimums, but with case 2 the temperature has a much smoother evolution over time, with nearly no significant lows. This increases the COP of the heat pump, despite operating on a partial load. The grout-filled volume plots (named PCM Average Temperature) show the same qualitative behaviour as the work fluid, operating within the same temperature range, with a much less pronounced temperature drop at the eight hour mark, unlike the on/off regimen. Regarding case 3, the heat transfer fluid registers higher overall temperatures compared with cases 1 and 2. These temperatures are important to select PCMs with an appropriate operation temperature to fill the cylinders as these cases provide the base line for the following cases.

Fig. 7 shows for cases 4, 5 and 6 how the phase change process progresses as well as the solidus and liquidus temperatures for the currently simulated PCM, that for the specific cases it is the same, PCM A. The phase change temperature was selected based on the previously simulated cases. Fig. 8 illustrates and compares the absolute difference for the outlet temperature for cases 1 to 3 and their respective PCM counterparts, cases 4, 5 and 6, to visualise how the PCM influences the heat exchange within the borehole. The results show that in all the cases, 4 to 6, the PCM only partially changes phase, using approximately 4.0, 3.5, and 2.5 kWh, respectively, of the total energy stored (10.05 kWh), and while its stored energy is not completely used, the energy still allows for a stabilising effect on the borehole behaviour. However, this effect has little impact on the overall temperature evolution of the inlet and outlet temperatures of the work fluid, being at almost the same temperatures as cases 1 to 3, as seen in Fig. 8. In case 1 versus case 4 shows a temperature variation on average less than 0.15%, with even less variation concerning the case 2 and 3 relative to cases 5 and 6 respectively, with temperature differences below 0.02% for both. The reason for the larger variation for case 1 versus case 4 relates to the larger temperature oscillations that the On/Off system brings due to its mode of operation; the others have a much smoother operation thus less drastic fluctuations. Another related result is that despite the low effect, it is proved that using the PCMs in the boreholes has a positive effect on thermal performance of the system. Further elaborating, it is possible to see that in all the three cases, when the system was not operating the PCMs started to recharge from the surrounding soil, albeit not completely, consequence of the limited thermal conductivity of the PCMs and their encapsulation. In a system with thermal energy storage the time frame possible for the geothermal heat pump to be inactive can be extended without interrupting the energy being delivered to the building. Therefore, the recovery time for the PCMs can be extended when compared with a regular heating system with no thermal storage. Another relevant conclusion that can be drawn from these simulated cases is that the inverter technology makes for a much smoother operation, keeping the PCMs' temperature from needlessly dropping too sharply, depleting its stored energy.

Fig. 9 showcases simulations 7, 8 and 9. For the stated cases, the PCMs tested were PCM B, C and D. Observing the results for 7 and 8 it can be gathered that the difference in latent heat, and as such the energy storage capacity, influences the PCM behaviour, with the mass fraction and average temperature shifting up or down when the latent heat increases or decreases respectively. Nevertheless, these alterations do not seem to have a significant influence on the inlet and outlet temperatures, shifting the overall temperatures by about 0.5 °C. In case

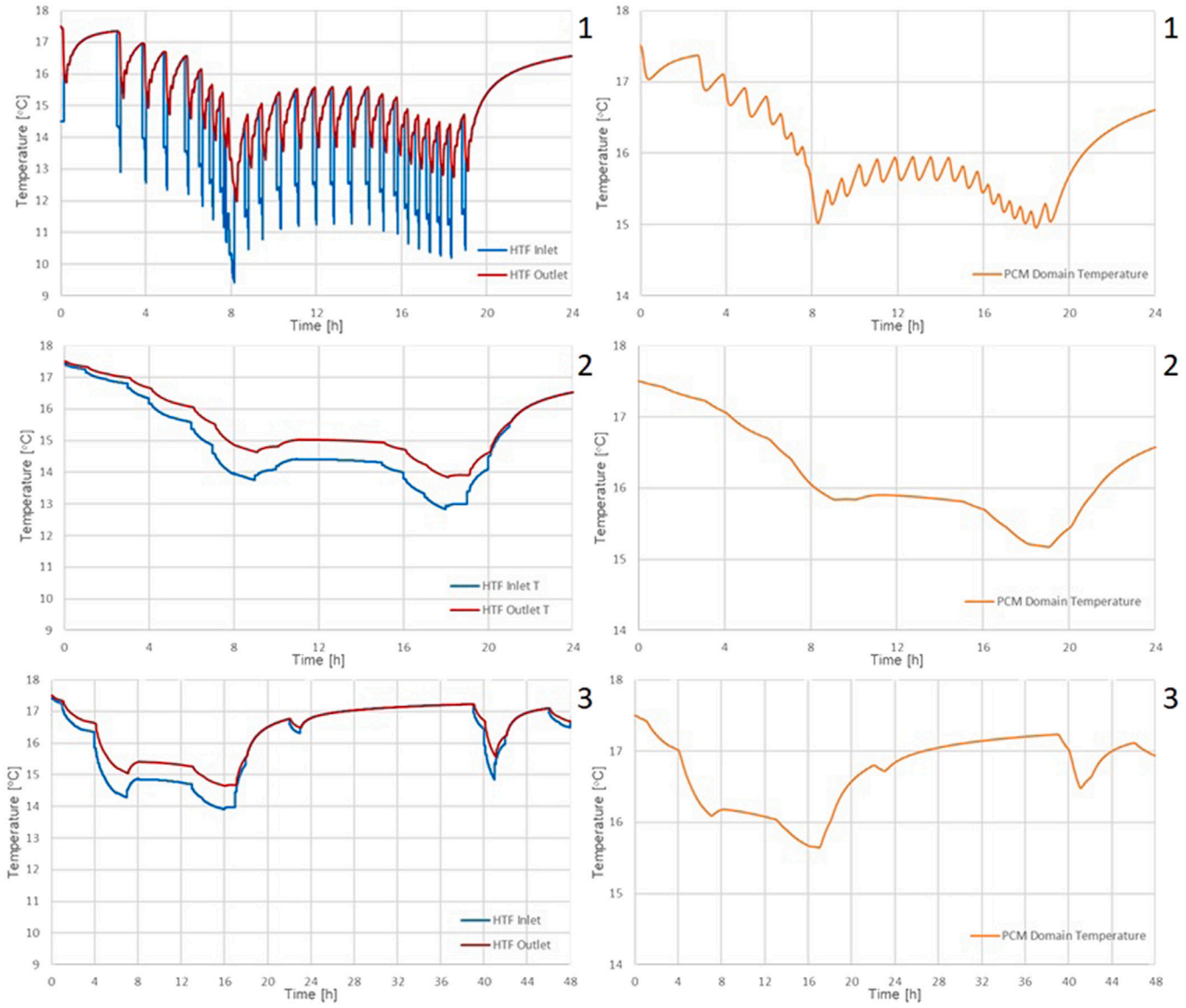

Fig. 6. Inlet and outlet temperatures of the HTF and temperature of the grout filled material for cases 1, 2 and 3.

9, shifting the PCMs operational range temperature up half a degree resulted in more usage taken out of the PCMs, both concerning the PCM behaviour and energy extracted from it, with the water temperatures shifting up as well.

3.2. Case comparison

Fig. 10 displays a comparison between cases 6, 7 and 8, comparing the effect of PCM A, PCM B and PCM C, that have the same operating temperatures for the phase change of the PCM but have a latent heat 25% below (case 7) and 25% above (case 8) PCM A. The results show that the latent heat influences the PCMs that solidify during the heat pump operation cycle, but as seen in Fig. 9 it has minimal impact on the overall heat transfer fluid temperatures or the PCM average temperature. The solidified fraction of PCM is proportional to the latent heat increase or decrease, with the lowest liquid mass fraction reaching around 70% for case 7, which has the lowest latent heat, while case 8, which has a higher latent heat, marginally drops to 80% for liquid mass fraction. Overall, in the cases on display, the PCMs never completely solidify when the heat pump is operating and the temperatures on display are minimally influenced.

Fig. 11 displays a comparison between cases 6 and 9, judging the influence of PCM A and PCM D, that have the same latent heat but a different operating temperature range, being 0.5 °C higher in case 9 than in case 6. Studying the results, this increase in temperature of PCM operation range (case 9) increases the mass of material that solidifies, and the overall temperatures of the borehole stabilised at a higher temperature, thus taking a greater advantage for the stored energy of the PCMs. The inlet and outlet temperatures on the work fluid are higher, which translates to an increase in the geothermal heat pump coefficient of performance as the temperature to be reached is not as low as in case 6. However, the results also show that in case 9, the PCMs are not able to reach the initial condition (recharged from the surrounding soil), only recharging up to 90% of the energy. This highlights the drawback of increasing the material operating temperature range, and also the low thermal conductivity of the overall storage medium (PCMs, encapsulation, grout and soil). Ideally the PCMs should be able to be cyclically recharged by the soil, over each operating cycle.

Fig. 12 showcases a simple comparison for cases 3 and 9, effectively comparing a 48-hour inverter heat pump operation cycle with no PCMs in the borehole (case 3) with a case that has the same operation cycle with PCM D (case 9). Analysing the data clearly showed the advantage of integrating PCMs in a borehole heat exchanger; the PCMs increase

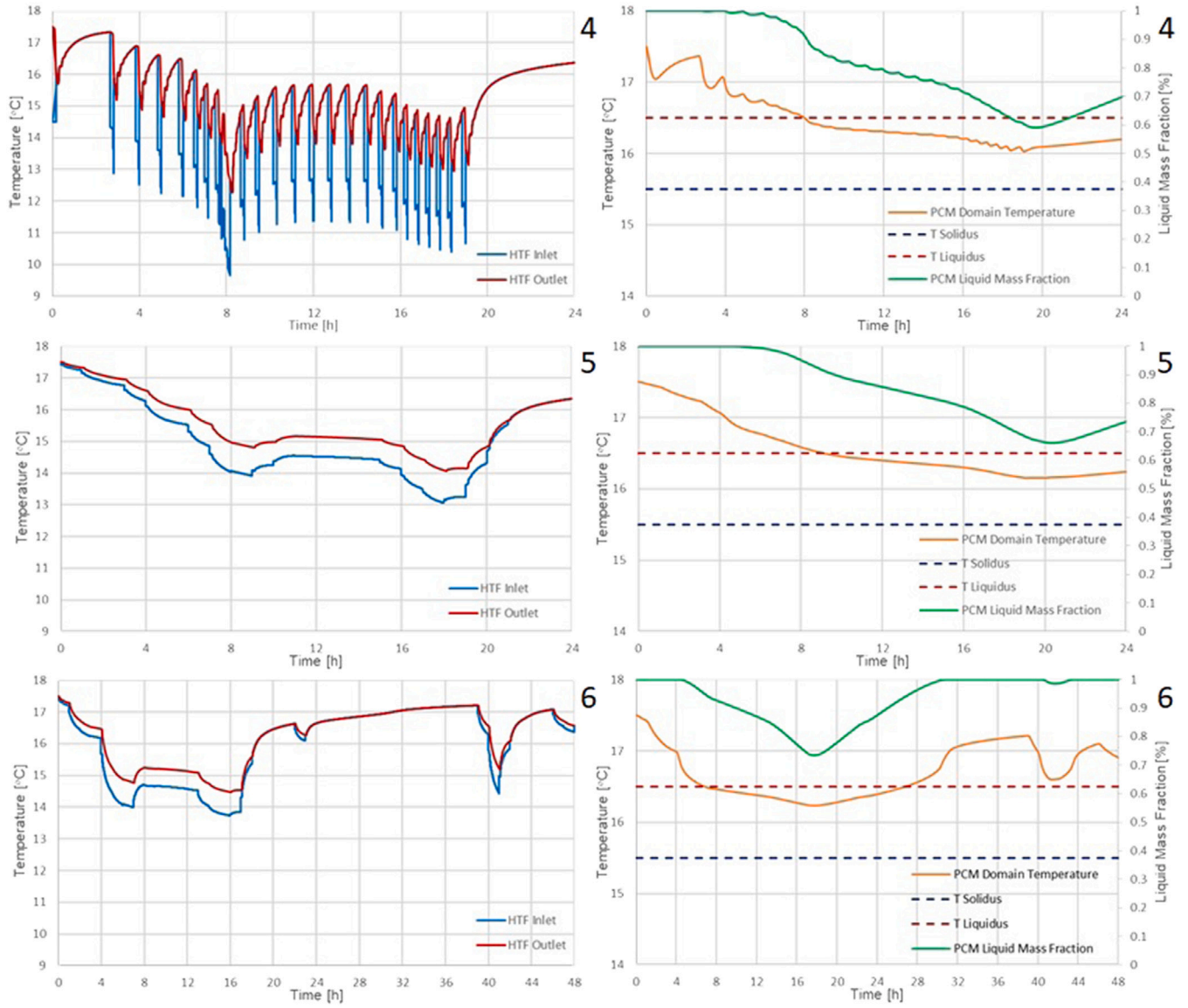

Fig. 7. Inlet and outlet temperatures of the HTF and PCM volume average temperature and liquid mass fraction for cases 4, 5 and 6.

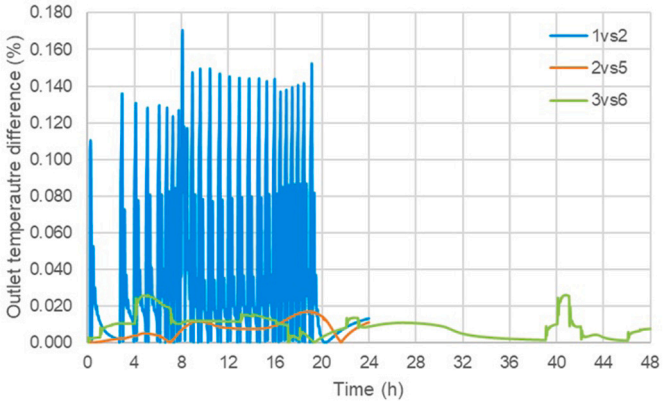

Fig. 8. Percentual absolute difference of the HTF outlet temperature comparing cases 1, 2 and 3 with cases 4, 5 and 6 respectively.

the thermal inertia of the borehole, stabilising its temperature when the geothermal heat pump is running. Generally, the temperatures registered for the heat transfer fluid are higher with PCMs in place; this contributes to the heat pump having an improved energy performance when operating, increasing energetic savings and decreased costs.

With all the results in mind, there are several more observations to be made about how the overall installation works regarding both PCM and the operation regimen. One point is that modifying and placing PCM into one of the "U" pipe sections of the Double "U" borehole without further modifications will be insufficient. Not only is there is limited volume to store PCM in to make a significant contribution to the overall process, but the way PCM is stored significantly limits their capacity to transfer their stored energy to the surroundings in a meaningful way. For a useful type of macro encapsulation to be used, other alternatives would have to be found. The consequences of these limitations can clearly be seen in almost negligible temperature variation when compared with the cases without PCM. Further evidence of the limitations of the encapsulation can also be seen in the mass fraction graphs, which shows that the PCMs are never fully discharged. These limitations not only concern the encapsulation and the PCMs' thermal conductivity limitations but also shows that if operation cycles are short (less than 24–36 h), there is little time for the soil to transfer back energy to the borehole/PCM in a timely manner to recharge. A factor

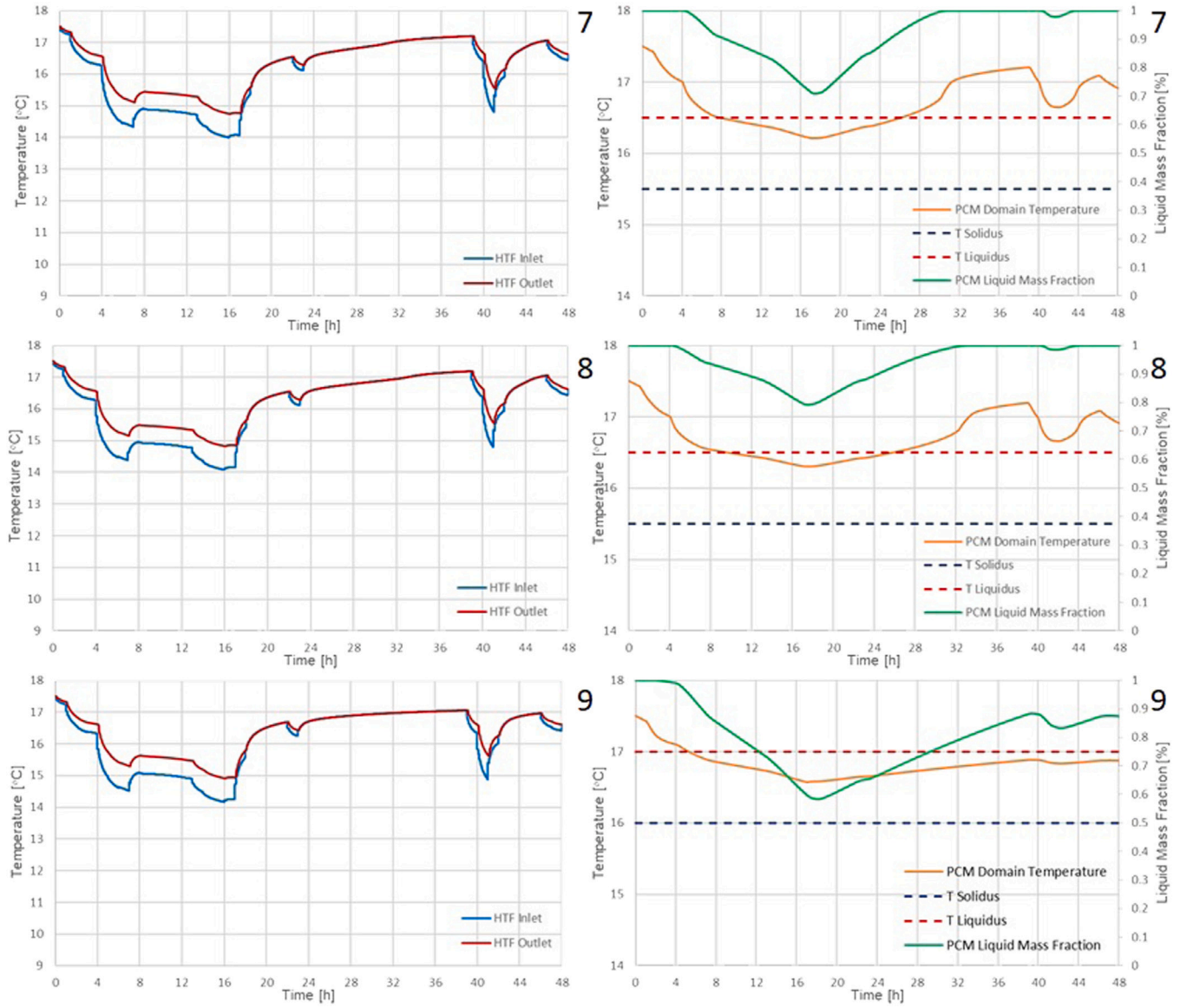

Fig. 9. Inlet and outlet temperatures of the HTF and PCM volume average temperature and liquid mass fraction for cases 7, 8 and 9.

in which the soil thermal conductivity also plays a part. One possible way to help overcome these issues, to a limited extent, would be to further change the PCMs' working temperatures. Concerning the usage of alternative PCM encapsulations (micro and nano-encapsulations) for mixing with grout material, the potential use of this application offers an attractive prospect as it has a simple implementation method and can provide a great benefit to the operating heating/cooling systems that rely on it, provided that it is well designed to match the thermal needs and soil conditions and does not suffer from PCM leaching from the encapsulation. Thus, further work should be carried out to develop this technology for implementation in a future solution.

4. Conclusions

This study conducted a series of computational fluid dynamics simulation cases to determine the influence of macro encapsulated PCMs in a borehole heat exchanger in association with a GSHP. The results showed that:

- Using the inverter technology smooths out the heat transfer fluid temperatures, decreasing the temperature difference by 36% relative to the On/Off system, thereby contributing to a more efficiently run geothermal heat pump. Coincidentally the On/Off system was the one that benefited more from the PCM application as the inverter adjusted better to required conditions.
- A higher PCM temperature operation range (16–17 °C instead of 15.5–16.5 °C) helps stabilise the temperatures at a higher baseline, but this incurs a drawback that prevents the material fully recovering in the heat pump down time, decreasing its temperature difference comparatively with the soil.
- While it underperformed for the studied parameters, with the case of the PCM On/Off system having an average maximum temperature difference of 0.15% between the case with and without PCM due to the system limitations. It is clear that the PCM application in the borehole has a stabilising function, with the strong influence of its temperature operational range. This improves the energy performance of the heat pump thus increasing savings.
- The limitations could be minimised if the PCM thermal conductivity could be successfully increased without relinquishing significant latent heat capacity. For instance, if the macro encapsulated PCMs were doped with high conductivity, stable nano particles that would improve the heat transfer to and from the PCM mass.

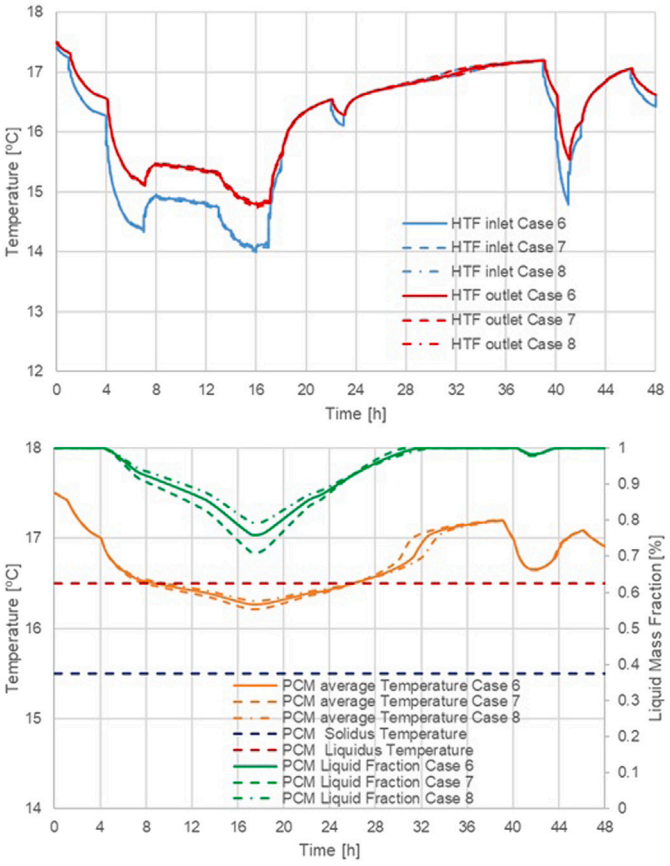

Fig. 10. Comparison of the inlet and outlet temperatures of the HTF and PCM volume average temperature and liquid mass fraction for cases 6, 7 and 8.

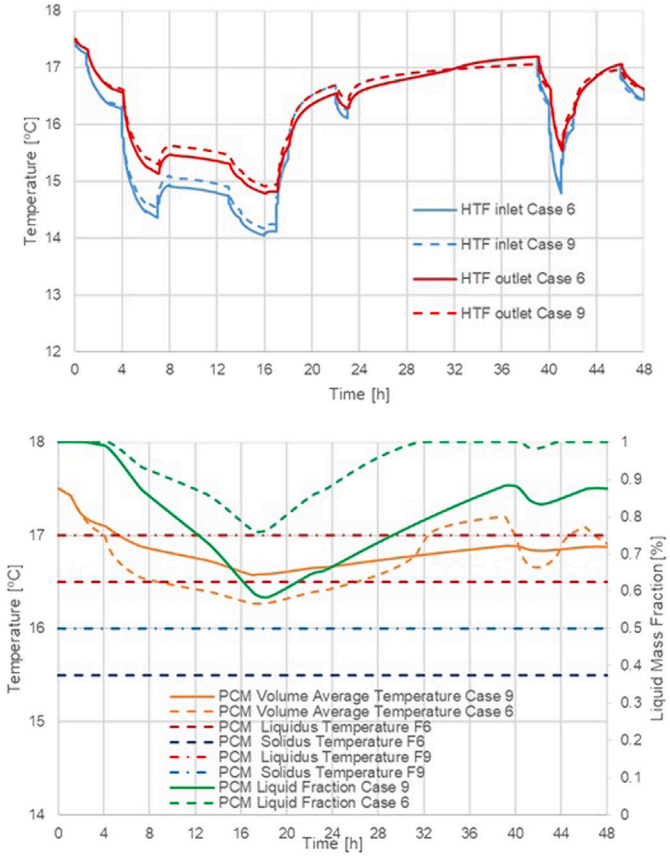

Fig. 11. Comparison of the inlet and outlet temperatures of the HTF and PCM volume average temperature and liquid mass fraction for cases 6 and 9.

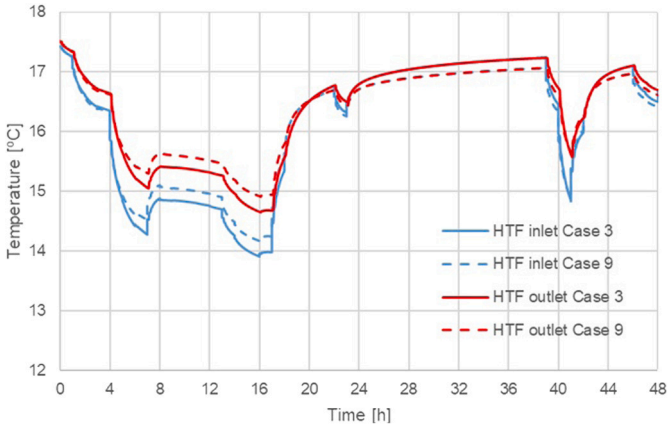

Fig. 12. Comparison of the inlet and outlet temperatures of the HTF for cases 3 and 9.

Alternatively, by using a different encapsulation method such as micro and nano encapsulation that does not leech PCM out.

- Additional work is needed to expand on and develop the technical solution and to verify the influence the PCMs have on the overall system and its operation modes over extended periods of use. It should be noted that should such an application as the one explored here be successfully developed it would result in shallower boreholes, which, given the nature of geothermal systems installation, would contribute significantly to reducing the installation costs and the overall cost of any thermal system coupled with it.

Declaration of competing interest

The authors declare that they have no known competing financial interests or personal relationships that could have appeared to influence the work reported in this paper.

Data availability

The authors do not have permission to share data.

Acknowledgements

This work was financially supported by the TESSe2b project that has received funding from the European Union's Horizon 2020 research and innovation programme under grant agreement No 680555. This article reflects only the authors' view and the European Commission is not responsible for any use that may be made of the information it contains. This publication was supported by the Polytechnic Institute of Setúbal, Portugal.

References

[1] J.-M. Durand, M.J. Duarte, P. Clerens, Joint EASE/EERA Recommendations for a European Energy Storage Technology Development Roadmap 2030, Tech. Rep., European Association for Storage of Energy and European Energy Research Alliance, Brussels, 2013.

[2] E. Douvi, C. Pagkalos, G. Dogkas, M.K. Koukou, V.N. Stathopoulos, Y. Caouris, M.G. Vrachopoulos, Phase change materials in solar domestic hot water systems: A review, Int. J. Thermofluids 10 (2021) 100075, http://dx.doi.org/10.1016/j.ijft.2021.100075, URL https://linkinghub.elsevier.com/retrieve/pii/S2666202721000136.

[3] Innovation Outlook: Thermal Energy Storage, Tech. Rep., IRENA, Abu Dhabi, 2020.

[4] F. Agyenim, N. Hewitt, P. Eames, M. Smyth, A review of materials, heat transfer and phase change problem formulation for latent heat thermal energy storage systems (LHTESS), Renew. Sustain. Energy Rev. 14 (2) (2010) 615–628, http://dx.doi.org/10.1016/j.rser.2009.10.015, URL https://linkinghub.elsevier.com/retrieve/pii/S1364032109002469.

[5] A. Aljabr, A. Chiasson, A. Alhajjaji, Numerical modeling of the effects of micro-encapsulated phase change materials intermixed with grout in vertical borehole heat exchangers, Geothermics 96 (2021) 102197, http://dx.doi.org/10.1016/j.geothermics.2021.102197, URL https://linkinghub.elsevier.com/retrieve/pii/S0375650521001577.

[6] A. Alkhwildi, R. Elhashmi, A. Chiasson, Parametric modeling and simulation of Low temperature energy storage for cold-climate multi-family residences using a geothermal heat pump system with integrated phase change material storage tank, Geothermics 86 (2020) 101864, http://dx.doi.org/10.1016/j.geothermics.2020.101864, URL https://linkinghub.elsevier.com/retrieve/pii/S0375650519304559.

[7] M. Bottarelli, E. Baccega, S. Cesari, G. Emmi, Role of phase change materials in backfilling of flat-panels ground heat exchanger, Renew. Energy 189 (2022) 1324–1336, http://dx.doi.org/10.1016/j.renene.2022.03.061, URL https://linkinghub.elsevier.com/retrieve/pii/S0960148122003445.

[8] B.B. Dehghan, A. Sisman, M. Aydin, Optimizing the distance between boreholes with helical shaped ground heat exchanger, 2015.

[9] Z.S. Qi, Q. Gao, Y. Liu, Y. Yan, J.D. Spitler, The performance improvements of a ground-coupled heat pump system for both building heating and cooling modes, Adv. Mater. Res. 354–355 (2011) 807–810, http://dx.doi.org/10.4028/www.scientific.net/AMR.354-355.807, URL https://www.scientific.net/AMR.354-355.807.

[10] M. Mahmoud, M. Ramadan, K. Pullen, M.A. Abdelkareem, T. Wilberforce, A.-G. Olabi, S. Naher, A review of grout materials in geothermal energy applications, Int. J. Thermofluids 10 (2021) 100070, http://dx.doi.org/10.1016/j.ijft.2021.100070, URL https://www.sciencedirect.com/science/article/pii/S2666202721000082.

[11] C.N. Elias, V.N. Stathopoulos, A comprehensive review of recent advances in materials aspects of phase change materials in thermal energy storage, Energy Procedia 161 (2019) 385–394, http://dx.doi.org/10.1016/j.egypro.2019.02.101, Proceedings of the 2nd International Conference on Sustainable Energy and Resource Use in Food Chains including Workshop on Energy Recovery Conversion and Management; ICSEF 2018, 17 – 19 October 2018, Paphos, Cyprus. URL https://www.sciencedirect.com/science/article/pii/S1876610219311816.

[12] W. Yang, R. Xu, B. Yang, J. Yang, Experimental and numerical investigations on the thermal performance of a borehole ground heat exchanger with PCM backfill, Energy 174 (2019) 216–235, http://dx.doi.org/10.1016/j.energy.2019.02.172, URL https://linkinghub.elsevier.com/retrieve/pii/S0360544219303780.

[13] B. Koçak, A.I. Fernandez, H. Paksoy, Review on sensible thermal energy storage for industrial solar applications and sustainability aspects, Sol. Energy 209 (2020) 135–169, http://dx.doi.org/10.1016/j.solener.2020.08.081, URL https://linkinghub.elsevier.com/retrieve/pii/S0038092X20309208.

[14] O. Okogeri, V.N. Stathopoulos, What about greener phase change materials? A review on biobased phase change materials for thermal energy storage applications, Int. J. Thermofluids 10 (2021) 100081, http://dx.doi.org/10.1016/j.ijft.2021.100081, URL https://linkinghub.elsevier.com/retrieve/pii/S2666202721000197.

[15] A. Sharma, C. Chen, Solar water heating system with phase change materials, Int. Rev. Chem. Eng. 1 (4) (2009) 297–307.

[16] A. Sharma, V. Tyagi, C. Chen, D. Buddhi, Review on thermal energy storage with phase change materials and applications, Renew. Sustain. Energy Rev. 13 (2) (2009) 318–345, http://dx.doi.org/10.1016/j.rser.2007.10.005, URL https://linkinghub.elsevier.com/retrieve/pii/S1364032107001402.

[17] M. Mousa, A. Bayomy, M. Saghir, Long-term performance investigation of a GSHP with actual size energy pile with PCM, Appl. Therm. Eng. 210 (2022) 118381, http://dx.doi.org/10.1016/j.applthermaleng.2022.118381, URL https://linkinghub.elsevier.com/retrieve/pii/S1359431122003386.

[18] X. Zhang, M. Zhao, L. Liu, C. Huan, Y. Zhao, C. Qi, K.-I. Song, Numerical simulation on heat storage performance of backfill body based on tube-in-tube heat exchanger, Constr. Build. Mater. 265 (2020) 120340, http://dx.doi.org/10.1016/j.conbuildmat.2020.120340, URL https://linkinghub.elsevier.com/retrieve/pii/S095006182032345X.

[19] A. Pandey, M. Hossain, V. Tyagi, N. Abd Rahim, J.A. Selvaraj, A. Sari, Novel approaches and recent developments on potential applications of phase change materials in solar energy, Renew. Sustain. Energy Rev. 82 (2018) 281–323, http://dx.doi.org/10.1016/j.rser.2017.09.043, URL https://linkinghub.elsevier.com/retrieve/pii/S1364032117312972.

[20] C. Vella, S.P. Borg, D. Micallef, The effect of shank-space on the thermal performance of shallow vertical U-tube ground heat exchangers, Energies 13 (3) (2020) 602, http://dx.doi.org/10.3390/en13030602, URL https://www.mdpi.com/1996-1073/13/3/602.

[21] M. Mousa, A. Bayomy, M. Saghir, Phase change materials effect on the thermal radius and energy storage capacity of energy piles: Experimental and numerical study, Int. J. Thermofluids 10 (2021) 100094, http://dx.doi.org/10.1016/j.ijft.2021.100094, URL https://www.sciencedirect.com/science/article/pii/S266620272100032X.

[22] J.M. Mahdi, E.C. Nsofor, Solidification enhancement of PCM in a triplex-tube thermal energy storage system with nanoparticles and fins, Appl. Energy 211 (2018) 975–986, http://dx.doi.org/10.1016/j.apenergy.2017.11.082, URL https://linkinghub.elsevier.com/retrieve/pii/S0306261917316811.

[23] I. Sarani, S. Payan, S. Nada, A. Payan, Numerical investigation of an innovative discontinuous distribution of fins for solidification rate enhancement in PCM with and without nanoparticles, Appl. Therm. Eng. 176 (2020) 115017, http://dx.doi.org/10.1016/j.applthermaleng.2020.115017, URL https://linkinghub.elsevier.com/retrieve/pii/S1359431119358107.

[24] M. Longeon, A. Soupart, J.-F. Fourmigué, A. Bruch, P. Marty, Experimental and numerical study of annular PCM storage in the presence of natural convection, Appl. Energy 112 (2013) 175–184, http://dx.doi.org/10.1016/j.apenergy.2013.06.007, URL https://linkinghub.elsevier.com/retrieve/pii/S030626191300514X.